nature plants

Article

https://doi.org/10.1038/s41477-024-01700-4

Molecular-level carbon traits underlie the multidimensional fine root economics space

Received: 25 October 2023

Accepted: 15 April 2024

Published online: 13 May 2024

Check for updates

Mengke Wang[1,2], Deliang Kong[3] ✉, Xiaohan Mo[4], Yinghui Wang[1,2], Qingpei Yang[3], Paul Kardol[5,6], Oscar J. Valverde-Barrantes[7], Myrna J. Simpson[8], Hui Zeng[4], Peter B. Reich[9,10,11], Joana Bergmann[12], Nishanth Tharayil[13] & Junjian Wang[1,2] ✉

Carbon influences the evolution and functioning of plants and their roots. Previous work examining a small number of commonly measured root traits has revealed a global multidimensionality of the resource economics traits in fine roots considering carbon as primary currency but without considering the diversity of carbon-related traits. To address this knowledge gap, we use data from 66 tree species from a tropical forest to illustrate that root economics space co-varies with a novel molecular-level traits space based on nuclear magnetic resonance. Thinner fine roots exhibit higher proportions of carbohydrates and lower diversity of molecular carbon than thicker roots. Mass-denser fine roots have more lignin and aromatic carbon compounds but less bioactive carbon compounds than lighter roots. Thus, the transition from thin to thick fine roots implies a shift in the root carbon economy from 'do-it-yourself' soil exploration to collaboration with mycorrhizal fungi, while the shift from light to dense fine roots emphasizes a shift from acquisitive to conservative root strategy. We reveal a previously undocumented role of molecular-level carbon traits that potentially undergird the multidimensional root economics space. This finding offers new molecular insight into the diversity of root form and function, which is fundamental to our understanding of plant evolution, species coexistence and adaptations to heterogeneous environments.

Variation in root functional traits is crucial for plant survival and coexistence in heterogeneous environments. These variations have been represented as a multidimensional, global root economics space[1–4] that reflects plants' ecological strategies under natural selection. In one such representation with four commonly measured root functional traits, this economics space has two dimensions: one with a negative correlation between root nitrogen content and root tissue density. This could be interpreted as a trade-off between resource acquisition and conservation strategies[2,5,6], that is, the 'fast–slow' plant economics spectrum. The other dimension exhibits a negative correlation between root diameter and specific root length (the root length per unit mass), highlighting a 'collaboration gradient' with mycorrhizal fungi in soil nutrient exploration, from 'do-it-yourself' by thin fine roots with high specific root length to 'outsourcing' of resource acquisition to mycorrhizae for thick fine roots[2]. Nonetheless, the root economics space is still being fully elucidated[1,4], and the intricate connections to physiological functions are an important knowledge gap that needs to be filled to improve understanding of the diversity of root form and function. Moreover, despite these recent advances in understanding the carbon-focused root economics space, there have been a limited number of root traits considered and none related to root carbon chemistry per se.

Carbon compounds are the fundamental building blocks of plants at the organismal, cellular and molecular levels. Since the assimilation

A full list of affiliations appears at the end of the paper. ✉e-mail: deliangkong1999@126.com; wangjj@sustech.edu.cn

of carbon is a metabolically expensive process, plants are faced with the need to optimize the investment of limited carbon compounds[7,8]. Following the definition of 'functional traits' in ref. 9, we define a new term, 'carbon traits', as the content, composition and diversity of carbon compounds or carbon functional groups that influence plant performance and fitness. However, the impact of carbon traits on root trait space has rarely been described[10]. This is partly due to the perception that carbon contents of fine roots are very similar across species (usually 39–45% of dry root mass), hence this 'bulk trait' cannot be meaningfully correlated with other traits[11]. However, this perception is potentially misleading as the macroscale carbon content masks the diversity of organic compounds in plant roots[8]. Compared with the relatively stable total root carbon content, variation in the molecular composition of carbon across plant species is much higher and has a stronger association with root architecture[12] and ancestry[13,14]. Root decomposition dynamics and root ecological strategies are probably dependent on the carbon composition of root rather than the total carbon content[15–17]. However, in previous treatments of the current root economics space, no connection has been made between compositional carbon traits and commonly measured root functional traits.

Plants assimilate carbon dioxide as carbohydrates (rich in *O*-alkyl carbon) through photosynthesis. A substantial portion of carbohydrates is allocated towards the synthesis of cell walls. Notably, these carbohydrates are predominantly deposited as macromolecule polymers (cellulose and hemicellulose) and encapsulate the protoplasts of root cells, supporting root elongation and root-tip growth[18–20]. Other simple carbohydrates serve as vital carbon sources and energy reservoirs, essential for metabolic processes in plants. In addition, polyphenolic and hydrophobic compounds (rich in aromatic and *O*-aromatic carbon), such as lignin and suberin, are deposited in cell walls and increase root mechanical strength and tissue density[21–23], while other polyphenols, including tannins and flavonoids, protect roots from pathogen infection[24,25]. However, these compounds cannot be reused in plant metabolism and represent a dead end for metabolic pathways[26]. Furthermore, plants also biosynthesize various biomolecules containing alkyl, *N*-alkyl/methoxy, and carbonyl and carboxyl carbon, such as lipids, nucleic acids and proteins. These biomolecules are crucial components of protoplasts, playing a vital role in shaping the structure, facilitating signal transduction and maintaining the metabolic activity of root cells[24,27]. Despite shedding light on how the form and function of roots adapt to changing environments, the root economics space overlooks the role of root carbon composition in shaping root adaptive strategies. A better understanding of how root carbon traits relate to commonly measured root functional traits will provide new insights into the biochemical mechanisms underlying the multidimensionality of plant roots and the functioning of individual plants in ecosystems.

Previous studies have attempted to determine compound-specific root chemical composition and diversity, especially of the carbon traits[14,28]. Due to the high complexity and challenge in characterizing molecular-level root chemical composition, one complementary approach is to assess chemical diversity on the basis of chemical functional groups. Solid-state ^{13}C nuclear magnetic resonance (NMR) is an advanced technique that can provide structural information on carbon functional groups[29,30]. With this technique, we can detect key carbon functional groups such as alkyl, *N*-alkyl/methoxy, *O*-alkyl, di-*O*-alkyl, aromatic, *O*-aromatic, and carbonyl and carboxyl carbon, and root structural carbon trait diversity (H'_{RSC}) can also be calculated (see Methods and Table 1), thus providing a compound-agnostic characterization of the chemical space.

In total, we analysed eight molecular-level carbon traits plus total carbon content and four commonly measured root functional traits (root diameter, specific root length, root tissue density and root nitrogen content) for mature trees of 66 tropical woody species spanning over three major angiosperm clades (magnoliids, asterids and rosids). We abstained from measuring additional traits pertinent to root economics space, such as root respiration[31] and root lifespan[32]. These traits are presumed to bear some degree of association with carbon traits[5,10]. However, due to practical challenges inherent in field measurements and the scarcity of data within root trait databases, extrapolating these root trait datasets alongside carbon trait data to a global scale presents considerable difficulty. Therefore, these traits were not included in our study. All samples were collected from a tropical seasonal rainforest in Xishuangbanna, one of the regions with the richest tree species in China (details in Methods, Extended Data Fig. 1 and Supplementary Table 1).

We first hypothesize the existence of a two-dimensional (2D) space comprising the molecular-level carbon traits. In this carbon traits space, defensive carbon (for example, aromatic and *O*-aromatic carbon) persists stably due to their non-reusable nature and thus should be balanced with carbon enriched in *N*-alkyl/methoxy and carbonyl and carboxyl, representative of high physiological activity. In addition, considering that *O*-alkyl carbon is the primary source of carbon and energy for almost all metabolic processes, it should be treated as independent of the aforementioned dimensions. Second, we hypothesize that there is a root functional traits space that incorporates the commonly measured root functional traits and molecular-level carbon traits. Specifically, alongside the 'collaboration gradient' dimension, we expect that thinner fine roots, which must penetrate and explore the soil on their own, will invest more in carbohydrates built from *O*-alkyl carbon to enhance their tensile mechanics. Furthermore, alongside the acquisition–conservation dimension, denser fine roots usually accompanied by low nitrogen content and hence lower respiration rates[33,34], are expected to have more aromatic and *O*-aromatic denser carbon structures but less *N*-alkyl carbon structures.

Table 1 | Assignments of regions in solid-state ^{13}C NMR spectra

Chemical shift region (ppm)	Name	Assignment
0–45	alkyl	Terminal methyl groups, methylene groups in aliphatic rings and chains
45–60	*N*-alkyl/methoxy	Methoxyl groups and C-6 of carbohydrates and sugars, C-α of most amino acids
60–95	*O*-alkyl	Carbohydrate-derived structures (C-2 to C-5) in hexoses, C-α of some amino acids
95–110	di-*O*-alkyl	Anomeric carbon of carbohydrates, C-2, C-6 of syringyl units of lignin
110–145	aromatic	Aromatic C-H carbons, guaiacyl C-2, C-6 in lignin, olefinic carbons
145–165	*O*-aromatic	Aromatic COR or CNR groups
165–210	carbonyl and carboxyl	Carboxyl/carbonyl/amide carbons

Results

Phylogenetic influence on root traits

The species set showed phylogenetic effects on many functional traits, but not for root tissue density, root carbon concentration, carbonyl and carboxyl carbon, and H'_{RSC}. For example, roots of species of magnoliids were generally thick with low specific root length and *O*-alkyl carbon, while more recent lineages, such as rosids, showed the opposite pattern (Fig. 1). Compared with the commonly measured root functional traits in the 'collaboration gradient' (root diameter and specific root length), all the molecular-level carbon traits showed weaker phylogenetic signals (Fig. 1 and Supplementary Table 2). This suggests that root diameter and specific root length are more affected by the common ancestor, whereas the carbon traits are more sensitive to impacts from the microenvironment. Consequently, plant roots may have greater

https://doi.org/10.1038/s41477-024-01700-4

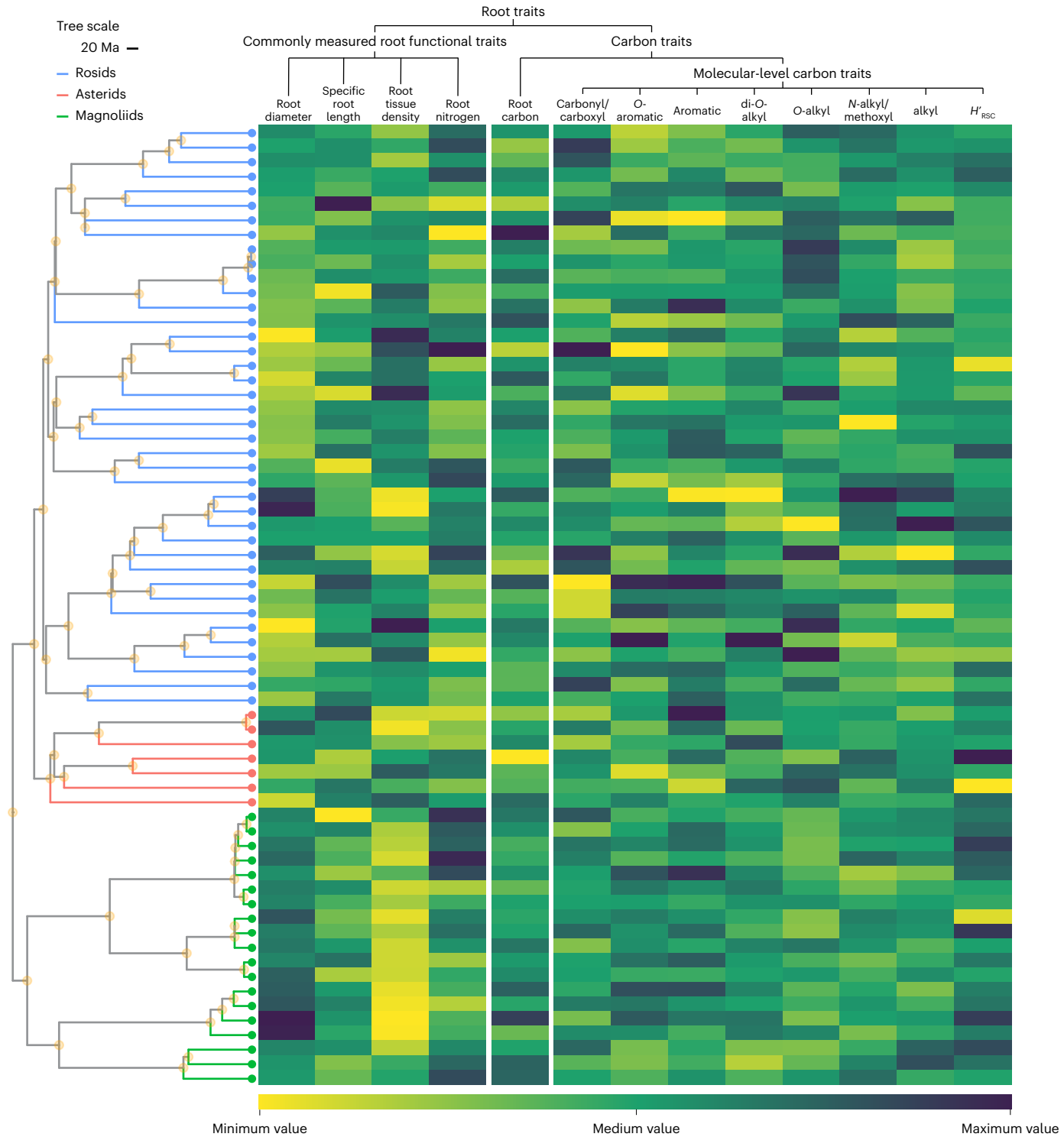

Fig. 1 | Phylogenetic relationships and 13 root traits for 66 tropical tree species. Phylogenetic tree of 66 species (left) with accompanying standardized species mean trait values (right) of 13 traits, ranging from low (yellow) to medium (green) to high (blue). The 13 root traits comprise four commonly measured functional traits (root diameter, specific root length, root tissue density and root nitrogen content) and 9 carbon traits, including total root carbon content and 8 molecular-level structural carbon traits. The molecular-level structural carbon traits were analysed via solid-state ^{13}C NMR and include alkyl, *N*-alkyl/methoxy, *O*-alkyl, di-*O*-alkyl, aromatic, *O*-aromatic, and carbonyl and carboxyl carbon, which were restricted within chemical shifts of 0–45, 45–60, 60–95, 95–110, 110–145, 145–165 and 165–210 ppm, respectively, in the ^{13}C NMR spectra. The major biochemical molecules are shown in Table 1. Root structural carbon trait diversity (H'_{RSC}) was calculated for each species using the Shannon diversity index (see Methods and Supplementary Table 1 for detailed information).

plasticity to modify aspects of key biomolecules rather than morphology in response to environmental changes[35,36]. The divergence of these traits in the phylogenetic signal further hints at a notable role of molecular-level carbon traits in driving root ecological strategies.

Two-dimensional root economics space

Using principal component analysis (PCA) of the four commonly measured functional traits, we found a 2D space that explains 85% of the variation (Fig. 2a and Supplementary Table 3). The first dimension is composed

https://doi.org/10.1038/s41477-024-01700-4

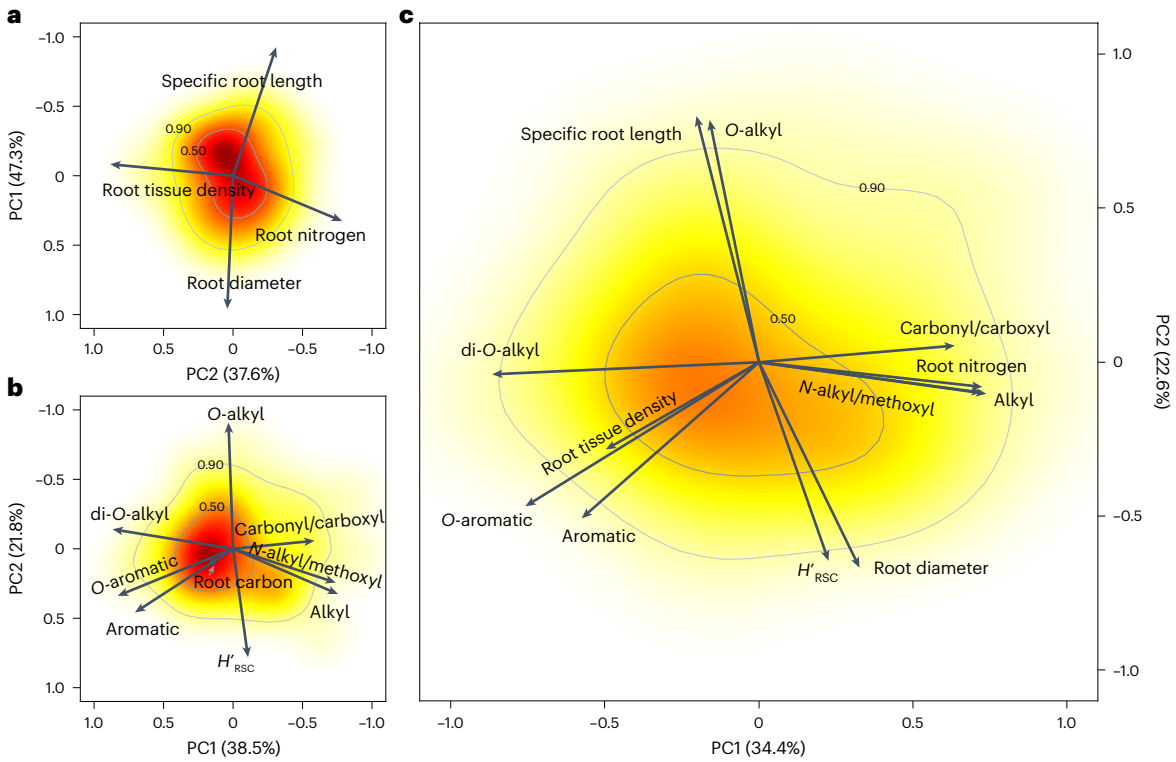

Fig. 2 | Coordination between the 2D root functional trait spaces and the molecular-level root carbon traits. PCA-based distribution of tropical tree species ($n = 66$) in root functional trait space, defined by commonly measured root functional traits and root carbon traits. **a**, Root economic traits space. **b**, Root carbon traits space, including total root carbon content and molecular-level carbon traits. **c**, Integrating both commonly measured root functional traits and molecular-level carbon traits in the 2D root functional traits space. The colour gradient indicates species occurrence probability in the traits space defined by principal components 1 and 2 (PC1 and PC2), with red indicating high occurrence and white indicating low occurrence. Contour lines indicate 0.50 and 0.90 quantiles. The commonly measured root functional traits are root diameter, specific root length, root tissue density and root nitrogen content. The carbon traits include total root carbon content and 8 molecular-level carbon traits (alkyl, *N*-alkyl/methoxy, *O*-alkyl, di-*O*-alkyl, aromatic, *O*-aromatic, carbonyl/carboxyl and structural carbon trait diversity (H'_{RSC})).

of root diameter and specific root length, while the second dimension reflects the negative correlation between root nitrogen content and root tissue density. This trait space is similar to the current framework reported in ref. 2, having two primary dimensions as confirmed by Horn's parallel analysis (see Methods for details). For the first two principal components, the loadings of our fine-root traits (Supplementary Table 3) have a Pearson correlation of 0.974 with the loadings in the global root economics space of ref. 2 (reported in Supplementary Table 1 of their work).

Two-dimensional root carbon traits space

When focusing solely on root carbon traits, we also found a 2D carbon traits space (Fig. 2b and Supplementary Table 4). The first component, which accounts for 39% of the variance, is mostly defined by six carbon traits (positive loadings: *O*-aromatic, aromatic and di-*O*-alkyl C; negative loadings: alkyl, carbonyl and carboxyl, and *N*-alkyl/methoxy C). The carbon functional groups in positive loadings originate mainly from lignin- and suberin-derived phenols and tannins[27,29], the common physical and chemical defensive compounds thickening the cell walls and enhancing plant tissue rigidity and stress resistance[23,26]. The other carbon functional groups in negative loadings consist mainly of amino acids, aliphatic compounds and carbonyl-containing compounds (for example, quinones, ketones and aldehydes)[29,30]; species enriched in these compounds exhibit high physiological activity, usually corresponding to high nitrogen content, high metabolism and root signalling[27]. Therefore, the first component of the carbon traits may represent a trade-off between physiological activity and defence in roots.

The second component, which accounts for 22% of the total variance, is mostly defined by an inverse correlation between *O*-alkyl carbon and H'_{RSC} (Fig. 2b and Supplementary Table 4). The vast majority of *O*-alkyl carbon in fine roots arises from carbohydrates, especially cellulose and hemicellulose in the cell wall[21,27]. High cellulose and hemicellulose content may constrain mycorrhizal colonization because more investment is needed to decompose these carbon compounds by the mycorrhizal fungi during symbiosis with the roots[37,38]. On the other hand, great carbon trait diversity (for example, fatty acids, strigolactones and flavonoids) may facilitate the maintenance of symbiosis of the roots with more diverse mycorrhizal fungi[39,40]. Therefore, the second component, similar to the aforementioned 'collaboration gradient', may represent carbon investment for mycorrhizal association. In addition, total root carbon content had low loadings on both axes, indicating a decoupling between molecular-level carbon traits (for example, *O*-alkyl and aromatic carbon) and total root carbon content.

Coordination between root economics space and carbon traits space

By integrating both the commonly measured functional traits and the molecular-level carbon traits, we observed a new 2D traits space with a cumulative explanatory power of 57%, reflecting coordination between the two sets of traits (Fig. 3c, Extended Data Fig. 2 and Supplementary Table 5). Simulation analyses showed significant correlations for PC1 ($r = -0.487$, $P = 3.00 \times 10^{-5}$) and PC2 ($r = 0.425$, $P = 3.40 \times 10^{-4}$) of the two sets of traits (Extended Data Fig. 3), further demonstrating the close coupling between molecular-level carbon traits and the root economics space.

The strong negative correlation for the PC1 of the two trait sets (*O*-aromatic, aromatic, di-*O*-alkyl, carbonyl and carboxyl, *N*-alkyl/

https://doi.org/10.1038/s41477-024-01700-4

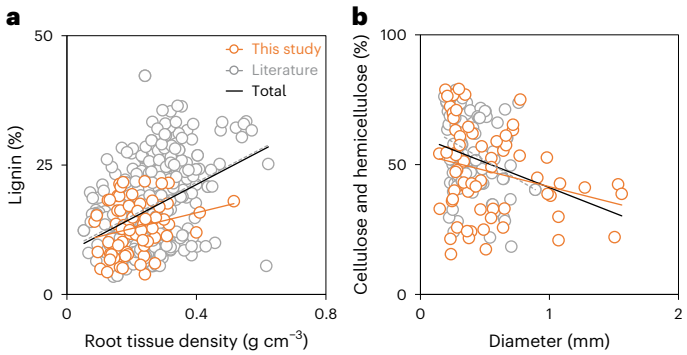

Fig. 3 | Relationships between cell wall chemistry and morphology in fine roots. a, Pearson correlation between root tissue density and lignin content for this study (in orange, $n = 66$, $r = 0.241$, $P = 0.051$), for global literature (in grey, $n = 315$, $r = 0.378$, $P = 4.09 \times 10^{-12}$) and for the total (in black, $n = 381$, $r = 0.392$, $P = 1.76 \times 10^{-15}$). **b**, Pearson correlation between root diameter and cellulose and hemicellulose content for this study (in orange, $n = 66$, $r = -0.252$, $P = 0.041$), for global literature (in grey, $n = 113$, $r = -0.314$, $P = 7.15 \times 10^{-4}$) and for the total (in black, $n = 179$, $r = -0.308$, $P = 2.75 \times 10^{-5}$). Significance was tested using a two-sided *t*-test. Literature data were collected from the Fine-Root Ecology Database (3.0)[62].

methoxy, and alkyl carbon vs root tissue density and root nitrogen concentration; $r = -0.487$, $P = 3.00 \times 10^{-5}$, Extended Data Fig. 3a) confirms that the 'conservation gradient' in the root economics space is coupled to the 'activity–defence' dimension in molecular-level carbon traits space (Fig. 2c). Specifically, root tissue density, *O*-aromatic, aromatic and di-*O*-alkyl carbon were loaded on the negative end of PC1 (Fig. 2c), indicating the role of these defensive compounds in contributing to high root tissue density[41,42]. These observations were corroborated by further analyses of our data and a global database, which demonstrate positive associations between root tissue density and lignin content (Fig. 3a). In addition, root nitrogen content and the carbon traits (for example, carbonyl and carboxyl, *N*-alkyl/methoxy and alkyl carbon) were loaded on the positive end of PC1 (Fig. 2c). Therefore, these carbon traits together with root nitrogen content indicate high physiological activity and, hence, an acquisitive strategy of the roots.

The strong correlations for the PC2 of the two trait sets (*O*-alkyl and H'_{RSC} vs root diameter and specific root length, $r = 0.425$, $P = 3.40 \times 10^{-4}$, Extended Data Fig. 3b) indicate that the collaboration gradient in the root economics space is coupled to the 'concentrated vs diversified investment' trade-off in the molecular-level carbon traits space (Fig. 2c). Although an intraspecific relationship between tensile strength and root diameter needs to be verified[43], fine roots with smaller diameter that invest in soil exploration probably require higher mechanical strength to overcome resistance encountered during root resource foraging[21,23]. Therefore, the prevalence of carbohydrates that were built from *O*-alkyl carbon in thinner fine roots may be due to the high axial stiffness, low bending stiffness and strong lateral bonding of the structural carbohydrates (that is, cellulose and hemicellulose) that contribute to high tensile mechanics[44].

Thicker fine roots showed a greater diversity of molecular-level carbon traits (H'_{RSC}) but a lower proportion of *O*-alkyl carbon (Fig. 2c). These roots primarily rely on mycorrhizal fungal partners for soil exploration and pathogen resistance[32], leading to the destruction and remodelling of the cell wall through symbiotic interactions between plants and microbes. For example, lytic enzymes can dissolve cellulose and hemicellulose[45], while newly synthesized specific polymers (for example, arabinogalactan or hydroxyproline-rich proteins and nodule-specific cysteine-rich peptides) can be deposited[46]. In addition, some fungal-specific compounds (for example, chitin, proteins and lipids) can be incorporated into the cell walls of the fine roots or adhere closely to the root cortex[47]. As fungi typically contain more di-*O*-alkyl, *N*-alkyl/methoxy and alkyl carbon, and less *O*-alkyl carbon than plants[48,49], the presence of more mycorrhizal hyphae in the root cortical tissue would result in a lower abundance of *O*-alkyl carbon. Hence, root diameter is inversely correlated with the percentage of *O*-alkyl carbon. This finding is supported by the significant negative correlation between root diameter and the sum of cellulose and hemicellulose contents based on data from our study and the global database (Fig. 3b). Meanwhile, the higher carbon traits diversity in thicker fine roots could be influenced by both roots and mycorrhizae. This is because higher root carbon diversity could facilitate symbiosis with more diverse mycorrhizal fungi bearing more diverse carbon compounds[39,40].

After removing the phylogenetic component from trait variation using a phylogenetically informed analysis, we tested the coordination between commonly measured root functional and carbon traits (Extended Data Fig. 4). This analysis indicated strong coordination between these traits even after controlling for phylogeny (as shown in Extended Data Figs. 4 and 5, and Supplementary Tables 3–5). This result provides strong evidence for the fundamental role of molecular-level carbon traits in generating multidimensionality in root traits at species level irrespective of the ancestry.

Furthermore, this study advances our understanding of niche differentiation among species in different phylogenetic clades. For example, thicker fine roots usually from magnoliids rather than rosids, tend to exhibit lower cellulose content but higher carbon trait diversity (Extended Data Fig. 6), making them advantageous in terms of higher pathogen resistance due to their higher colonization by mycorrhizal fungi[50,51]. This root trait syndrome may facilitate the dominance of the magnoliids in wet habitats with abundant pathogens.

Discussion

Our study demonstrates that the diverse economic strategies of individual roots are associated with and facilitated by multiple combinations of molecular-level root carbon traits. Compared with the widely used elemental-level carbon content or carbon-to- nitrogen ratio[11,52], the molecular-level carbon traits provide more direct support for the diversity of root forms and functions. Our findings that combine carbon traits with traditional root traits help explain how plant species are able to cope with the multidimensional and highly heterogeneous resource space in real-world ecosystems. For example, plant species with thinner fine roots tend to invest more in *O*-alkyl carbon to facilitate 'do-it-yourself' soil exploration (Fig. 4). In contrast, plant species bearing denser fine roots invest more in aromatics and less in nitrogenous or carbonyl-containing compounds (Fig. 4), which indicates a slower metabolism and higher defence of the roots. Moreover, we show that the coordination of certain carbon traits (for example, cellulose and lignin) with root morphological traits is similar whether using the current data or data from global databases (Fig. 3). Therefore, the coupling between molecular-level carbon traits and root economics space may be universal—an intriguing pattern that warrants further verification.

Here we reveal a novel 2D molecular-level root carbon traits trade-off that corresponds well to the two trade-offs of the four commonly measured root functional traits. This finding provides evidence for the role of the chemical composition of roots in shaping the 2D root functional traits space[53]. We acknowledge that the findings here, similar to the 'which comes first, the chicken or the egg' situation, cannot identify which comes first, the molecular-level carbon traits or the root functional traits space. The issue may however be clarified by investigating the composition of the root carbon compounds or genes for biosynthesis of specific carbon compounds along the evolutionary gradient back to the most primitive plant lineages[54,55]. Finally, we recognize the importance of considering other functional traits and whole-plant economics simultaneously. This entails the incorporation of carbon traits and economics pertaining not only to

https://doi.org/10.1038/s41477-024-01700-4

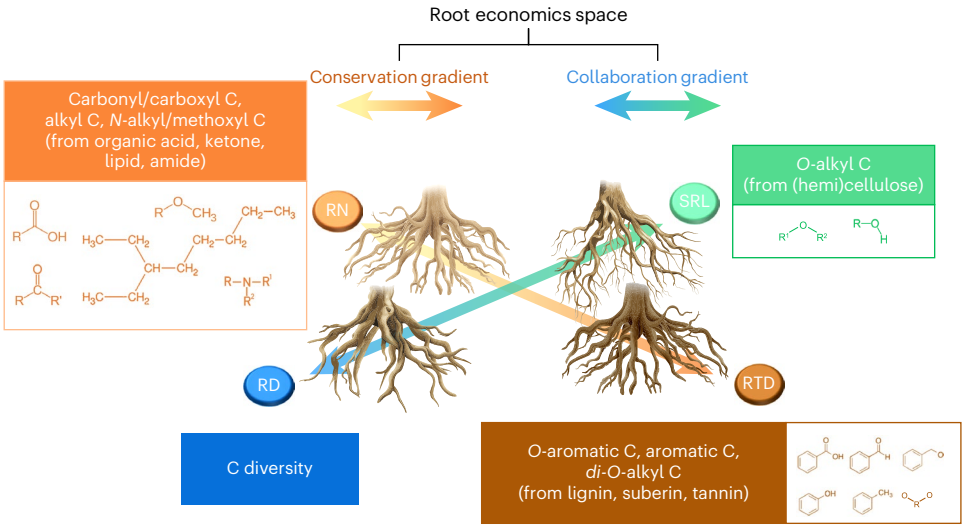

Fig. 4 | Conceptual framework of the 2D root functional traits space. This concept suggests that (1) lignin- and suberin-derived phenols and tannins may act as defensive compounds that enhance root tissue density (RTD), rigidity and stress resistance; (2) amino acids, aliphatic compounds and carbonyl-containing compounds (for example, quinones, ketones and aldehydes) facilitate high physiological activity, which corresponds to high nitrogen content (RN), high general metabolism and signalling of fine roots; (3) thinner fine roots with higher specific root length (SRL) invest more (hemi)cellulose for high mechanical strength to overcome resistance encountered from soil during root resource foraging; and (4) thicker fine roots with higher root diameter (RD) show a greater diversity of molecular-level carbon.

roots but also to plant leaves and stems. Such an approach is necessary to achieve a comprehensive understanding of the overarching pattern of whole-plant economics space and the associated trade-offs among molecule-level carbon traits.

Methods

Study site information

The study site is situated in Xishuangbanna, China (101.2° E, 21.95° N), within the Xishuangbanna National Nature Reserve (more than 2,400 km^2), which was established in 1958[56]. The study was conducted within a secondary forest in the reserve, which developed from a primary forest after minor human disturbances such as moderate logging for firewood. This site encompasses a tropical seasonal rainforest with an average annual precipitation of 1,428 mm and an average annual temperature of 22.5 °C. Its elevation ranges from 370 to 2,400 m above sea level. The soil type prevalent in this area is brick-red soil (Oxisol) derived from yellowish sandstone of the Cretaceous period. More details can be found in Supplementary Text 1.

Sampling and processing

We selected common woody species within the tropical forest, focusing on those with fine roots easily accessible from the surface soil. In total, 66 woody species that are most abundant in the canopy and subcanopy were selected. These species represent three major angiosperm lineages: rosids, asterids and magnoliids. Most species are native to the region and have grown in the forest for over 50 years. One species in our species pool, *Hevea brasiliensis*, is native to South America but was introduced to this area in the mid-twentieth century. Since then, it has become a common tree species in tropical forests in the region. In addition, *Betula alnoides*, *Acer laurinum* and *Celtis sinensis* are typically common in temperate forests; however, they also frequently occur in the tropical forest in our study area and other tropical forests in East Asia[57]. This selection process effectively minimized the potential confounding effects arising from climatic, geographical and soil variations, to ensure the representativeness and generalizability of the phylogeny of the observed patterns. These species represent 52 genera and 31 families belonging to three key angiosperm lineages: magnoliids, asterids and rosids (as shown in Extended Data Fig. 5 and Supplementary Table 1). Due to the prevalence of arbuscular mycorrhizal (AM) symbiosis in the majority of tree species within tropical forests, the tree species sampled in this study were predominantly of the AM mycorrhiza type (Supplementary Table 1).

To collect root samples, we followed the procedure outlined in a previous study[58]. For each species, we selected at least three mature plants (aged more than 30 years). We carefully excavated the surface soil (0–20 cm) at the base of the trees to expose the main lateral roots. We then cut root branches with intact terminal branch orders, collecting samples of the branches that included over 20 g of total fresh biomass of the first three-order roots, which play a crucial role in resource absorption[10].

To remove any soil adhering to the roots, we gently washed subsamples of each tree in deionized water. Next, we placed these samples immediately into plastic bags and kept them in a cooler for transport to the laboratory at Southern University of Science and Technology, Shenzhen, China. Upon arrival at the laboratory, we froze these samples at −20 °C until subsequent morphological and chemical analyses.

Chemical and morphological analysis

Carbon analysis. The roots were analysed for two types of carbon traits: total carbon content and molecular-level carbon traits. The samples were freeze-dried, carefully ground into fine powder, and all passed through a 200-mesh sieve for chemical analyses.

Total carbon content was determined using a Vario MACRO cube elemental analyser (Elementar).

Molecular-level carbon traits were analysed using solid-state ^{13}C NMR spectra acquired on a Bruker AVANCE III 600 spectrometer at a resonance frequency of 150.9 MHz with a 4 mm magic-angle spinning probe and spun at 12 kHz. We applied a contact time of 4 ms and recycle delay of 2 s for the ramp cross-polarization magic-angle spinning NMR measurements. The spectra were divided into seven main resonance regions according to the chemical shifts[59]: 0–45 ppm for alkyl carbon, 45–60 ppm for *N*-alkyl/methoxy carbon, 65–95 ppm for *O*-alkyl carbon, 95–110 ppm for di-*O*-alkyl carbon, 110–145 ppm for aromatic carbon, 145–165 ppm for *O*-aromatic carbon and 165–210 ppm for carboxyl and carbonyl carbon. Root structural carbon trait diversity was calculated using the Shannon diversity index[60]:

$$H'_{RSC} = -\sum_{i=1}^{7} p_i \times \ln p_i$$

where p_i is the proportion of the total abundances for the chemical shift of C_i.

Root cellulose, hemicellulose and lignin were analysed to verify cell wall carbon compound content derived from NMR-based carbon composition. The contents of hemicellulose and cellulose components and lignin components were detected following the Van Soest method[61] using a fibre analyser (ANKOM A2000i, Ankom).

Root economic trait measurements. More than four intact root branches per tree were taken for morphologic measurement. Root morphology parameters were acquired by root image analysis using Winrhizo software (2007 Pro version, Regent Instruments)[11]. The total nitrogen content was determined using a Vario MACRO cube elemental analyser (Elementar).

Literature data collection

We collected data from the Fine-Root Ecology Database (3.0)[62] and selected two series of data: Series 1 - root diameter (mm), cellulose content (%) and hemicellulose content (%); Series 2 - root tissue density (g cm^{-3}; also including the root dry matter content data according to ref. 63) and lignin content (%). A data record from the database would be selected if it contained all traits in one series. Series 1 data included 113 data records (75 known species and 5 unknown species) and Series 2 included 315 data records (128 known species and 62 unknown species). We did this to test the main findings of our experimental data regarding both carbon traits and morphological traits against global data.

Data analysis

We performed data analyses using R (v.4.1.1)[64]. To standardize plant species names and assign them to families, we used the Plant List (http://www.theplantlist.org/). Next, a dated molecular phylogeny was used to construct a phylogenetic tree using the package 'V. PhyloMaker'[65], although it may give a coarse phylogeny with poor tip resolution. Blomberg's *K* test was used to estimate phylogenetic signals for 13 traits. Blomberg's *K* was calculated using the package 'phytools' by assuming a Brownian motion model of evolution[66]. To examine the relationship between chemical and morphological traits, we constructed a Pearson's correlation matrix using the package Hmisc[67]. We square-root-transformed the variables to ensure homoscedasticity and normality of residual errors before performing the analysis.

To explore multiple root trait relationships, we performed a PCA using the 'factoextra' package[68]. Before conducting the PCA, we standardized the variable matrix to remove scale effects. Next, we estimated the species' probabilistic distribution in functional space using multivariate kernel density estimations in the 'ks' package[69]. We also examined the correlation between the loadings of our fine-root traits analysis and those reported in the literature for the first two principal components, using the 'vegan' package[70].

To investigate the independence between components 1 and 2, we conducted two PCAs for two different groups of variables (as shown in Fig. 2 and Extended Data Fig. 3). We designed a sampling distribution using 100,000 permutations of PC1 scores for each PCA and tested independence between components 1 and 2 using the 'ks' package[69]. We used a linear model to examine the covariation between content of cellulose and hemicellulose, and root diameter, as well as between lignin content and root tissue density. We performed this analysis using the package nlme[71]. Finally, we performed a phylogenetically informed PCA using the 'phyl.pca' function of the package 'phytools'[66,72].

Reporting summary

Further information on research design is available in the Nature Portfolio Reporting Summary linked to this article.

Data availability

All data supporting the findings of this study are available within this paper and its Supplementary Information. The raw data in this study are available via Figshare at https://doi.org/10.6084/m9.figshare.24218970 (ref. 73). Correspondence and requests for materials should be addressed to J.W. (wangjj@sustech.edu.cn). Literature data were extracted from Fine-Root Ecology Database 3.0 (https://roots.ornl.gov/)[62].

Code availability

The code utilized for this study is publicly available and is hosted in figshare at https://doi.org/10.6084/m9.figshare.24218970 (ref. 73).

References

1. Carmona, C. P. et al. Fine-root traits in the global spectrum of plant form and function. *Nature* **597**, 683–687 (2021).
2. Bergmann, J. et al. The fungal collaboration gradient dominates the root economics space in plants. *Sci. Adv.* **6**, eaba3756 (2020).
3. Diaz, S. et al. The global spectrum of plant form and function. *Nature* **529**, 167–171 (2016).
4. Weigelt, A. et al. An integrated framework of plant form and function: the belowground perspective. *New Phytol.* **232**, 42–59 (2021).
5. Reich, P. B. The world-wide 'fast-slow' plant economics spectrum: a traits manifesto. *J. Ecol.* **102**, 275–301 (2014).
6. Zhang, Y. et al. The worldwide allometric relationship in anatomical structures for plant roots. *Plant Divers.* **45**, 621–629 (2023).
7. Suseela, V. & Tharayil, N. Decoupling the direct and indirect effects of climate on plant litter decomposition: accounting for stress-induced modifications in plant chemistry. *Glob. Change Biol.* **24**, 1428–1451 (2018).
8. Weng, J. K., Lynch, J. H., Matos, J. O. & Dudareva, N. Adaptive mechanisms of plant specialized metabolism connecting chemistry to function. *Nat. Chem. Biol.* **17**, 1037–1045 (2021).
9. Violle, C. et al. Let the concept of trait be functional! *Oikos* **116**, 882–892 (2007).
10. McCormack, M. L. et al. Redefining fine roots improves understanding of below-ground contributions to terrestrial biosphere processes. *New Phytol.* **207**, 505–518 (2015).
11. Kong, D. et al. Leading dimensions in absorptive root trait variation across 96 subtropical forest species. *New Phytol.* **203**, 863–872 (2014).
12. Wang, J. J., Tharayil, N., Chow, A. T., Suseela, V. & Zeng, H. Phenolic profile within the fine-root branching orders of an evergreen species highlights a disconnect in root tissue quality predicted by elemental- and molecular-level carbon composition. *New Phytol.* **206**, 1261–1273 (2015).
13. Mueller, K. E., Polissar, P. J., Oleksyn, J. & Freeman, K. H. Differentiating temperate tree species and their organs using lipid biomarkers in leaves, roots and soil. *Org. Geochem.* **52**, 130–141 (2012).
14. Xia, M., Valverde-Barrantes, O. J., Suseela, V., Blackwood, C. B. & Tharayil, N. Coordination between compound-specific chemistry and morphology in plant roots aligns with ancestral mycorrhizal association in woody angiosperms. *New Phytol.* **232**, 1259–1271 (2021).
15. Sun, T. et al. Contrasting dynamics and trait controls in first-order root compared with leaf litter decomposition. *Proc. Natl Acad. Sci. USA* **115**, 10392–10397 (2018).
16. Suseela, V., Tharayil, N., Orr, G. & Hu, D. Chemical plasticity in the fine root construct of *Quercus* spp. varies with root order and drought. *New Phytol.* **228**, 1835–1851 (2020).
17. Poirier, V., Roumet, C. & Munson, A. D. The root of the matter: linking root traits and soil organic matter stabilization processes. *Soil Biol. Biochem.* **120**, 246–259 (2018).

18. Du, F. & Jiao, Y. L. Mechanical control of plant morphogenesis: concepts and progress. *Curr. Opin. Plant Biol.* **57**, 16–23 (2020).
19. Hofhuis, H. et al. Morphomechanical innovation drives explosive seed dispersal. *Cell* **166**, 222–233 (2016).
20. Coen, E. & Cosgrove, D. J. The mechanics of plant morphogenesis. *Science* **379**, eade8055 (2023).
21. Zhang, B., Gao, Y., Zhang, L. & Zhou, Y. The plant cell wall: biosynthesis, construction, and functions. *J. Integr. Plant Biol.* **63**, 251–272 (2021).
22. Burton, R. A., Gidley, M. J. & Fincher, G. B. Heterogeneity in the chemistry, structure and function of plant cell walls. *Nat. Chem. Biol.* **6**, 724–732 (2010).
23. Anderson, C. T. & Kieber, J. J. Dynamic construction, perception, and remodeling of plant cell walls. *Annu. Rev. Plant Biol.* **71**, 39–69 (2020).
24. Taiz, L., Zeiger, E., Møller, I. M. & Murphy, A. *Plant Physiology and Development* (Sinauer, 2015).
25. Weng, J.-K., Philippe, R. N. & Noel, J. P. The rise of chemodiversity in plants. *Science* **336**, 1667–1670 (2012).
26. Lux, A., Luxová, M., Abe, J. & Morita, S. Root cortex: structural and functional variability and responses to environmental stress. *Root Res.* **13**, 117–131 (2004).
27. Buchanan, B. B., Gruissem, W. & Jones, R. L. *Biochemistry and Molecular Biology of Plants* 2nd edn (Wiley Blackwell, 2015).
28. Xia, M., Valverde-Barrantes, O. J., Suseela, V., Blackwood, C. B. & Tharayil, N. Characterizing natural variability of lignin abundance and composition in fine roots across temperate trees: a comparison of analytical methods. *New Phytol.* **236**, 2358–2373 (2022).
29. Kögel-Knabner, I. ^{13}C and ^{15}N NMR spectroscopy as a tool in soil organic matter studies. *Geoderma* **80**, 243–270 (1997).
30. Hall, S. J., Ye, C. L., Weintraub, S. R. & Hockaday, W. C. Molecular trade-offs in soil organic carbon composition at continental scale. *Nat. Geosci.* **13**, 687–692 (2020).
31. Roumet, C. et al. Root structure–function relationships in 74 species: evidence of a root economics spectrum related to carbon economy. *New Phytol.* **210**, 815–826 (2016).
32. Ma, Z. et al. Evolutionary history resolves global organization of root functional traits. *Nature* **555**, 94–97 (2018).
33. Reich, P. B. et al. Scaling of respiration to nitrogen in leaves, stems and roots of higher land plants. *Ecol. Lett.* **11**, 793–801 (2008).
34. Hogan, J. A. et al. Functional variability in specific root respiration translates to autotrophic differences in soil respiration in a temperate deciduous forest. *Geoderma* **432**, 116414 (2023).
35. Zhang, H., Zhu, J., Gong, Z. & Zhu, J.-K. Abiotic stress responses in plants. *Nat. Rev. Genet.* **23**, 104–119 (2022).
36. Kelly-Bellow, R. et al. Brassinosteroid coordinates cell layer interactions in plants via cell wall and tissue mechanics. *Science* **380**, 1275–1281 (2023).
37. Genre, A., Lanfranco, L., Perotto, S. & Bonfante, P. Unique and common traits in mycorrhizal symbioses. *Nat. Rev. Microbiol.* **18**, 649–660 (2020).
38. Miyauchi, S. et al. Large-scale genome sequencing of mycorrhizal fungi provides insights into the early evolution of symbiotic traits. *Nat. Commun.* **11**, 5125 (2020).
39. Jiang, Y. et al. Plants transfer lipids to sustain colonization by mutualistic mycorrhizal and parasitic fungi. *Science* **356**, 1172–1175 (2017).
40. Banasiak, J., Jamruszka, T., Murray, J. D. & Jasinski, M. A roadmap of plant membrane transporters in arbuscular mycorrhizal and legume–rhizobium symbioses. *Plant Physiol.* **187**, 2071–2091 (2021).
41. Assefa, D., Godbold, D. L., Belay, B., Abiyu, A. & Rewald, B. Fine root morphology, biochemistry and litter quality indices of fast- and slow-growing woody species in Ethiopian highland forest. *Ecosystems* **21**, 482–494 (2018).
42. Zhao, Q. Lignification: flexibility, biosynthesis and regulation. *Trends Plant Sci.* **21**, 713–721 (2016).
43. Mao, Z. et al. Mechanical traits of fine roots as a function of topology and anatomy. *Ann. Bot.* **122**, 1103–1116 (2018).
44. Zhang, Y. et al. Molecular insights into the complex mechanics of plant epidermal cell walls. *Science* **372**, 706–711 (2021).
45. Chang, H. et al. Investigating lytic polysaccharide monooxygenase-assisted wood cell wall degradation with microsensors. *Nat. Commun.* **13**, 6258 (2022).
46. Rich, M. K., Schorderet, M. & Reinhardt, D. The role of the cell wall compartment in mutualistic symbioses of plants. *Front. Plant Sci.* **5**, 238 (2014).
47. Gow, N. A. R., Latge, J. P. & Munro, C. A. The fungal cell wall: structure, biosynthesis, and function. *Microbiol. Spectr.* https://doi.org/10.1128/microbiolspec.funk-0035-2016 (2017).
48. Kang, X. et al. Molecular architecture of fungal cell walls revealed by solid-state NMR. *Nat. Commun.* **9**, 2747 (2018).
49. Yoshida, M., Murai, T. & Moriya, S. ^{13}C NMR spectra of plant pathogenic fungi. *Agric. Biol. Chem.* **48**, 909–914 (1984).
50. Kalyuzhny, M., Lake, J. K., Wright, S. J. & Ostling, A. M. Pervasive within-species spatial repulsion among adult tropical trees. *Science* **381**, 563–568 (2023).
51. Hogan, J. A. et al. Root-associated fungal communities are influenced more by soils than by plant-host root traits in a Chinese tropical forest. *New Phytol.* **238**, 1849–1864 (2023).
52. Withington, J. M., Reich, P. B., Oleksyn, J. & Eissenstat, D. M. Comparisons of structure and life span in roots and leaves among temperate trees. *Ecol. Monogr.* **76**, 381–397 (2006).
53. Zhang, Y. et al. The origin of bi-dimensionality in plant root traits. *Trends Ecol. Evol.* **39**, 78–88 (2024).
54. Su, Y. et al. The evolutionary innovation of root suberin lamellae contributed to the rise of seed plants. *Nat Plants* **9**, 1968–1977 (2023).
55. Walker, T. W. N. et al. Leaf metabolic traits reveal hidden dimensions of plant form and function. *Sci. Adv.* **9**, eadi4029 (2023).
56. He, H. et al. Reference carbon cycle dataset for typical Chinese forests via colocated observations and data assimilation. *Sci. Data* **8**, 42 (2021).
57. Flora of China Editorial Committee. *Flora of China* (Science Press, 2004).
58. Guo, D. et al. Anatomical traits associated with absorption and mycorrhizal colonization are linked to root branch order in twenty-three Chinese temperate tree species. *New Phytol.* **180**, 673–683 (2008).
59. Nelson, P. N. & Baldock, J. A. Estimating the molecular composition of a diverse range of natural organic materials from solid-state ^{13}C NMR and elemental analyses. *Biogeochemistry* **72**, 1–34 (2005).
60. Meier, C. L. & Bowman, W. D. Links between plant litter chemistry, species diversity, and below-ground ecosystem function. *Proc. Natl Acad. Sci. USA* **105**, 19780–19785 (2008).
61. Van Soest, P. J. Use of detergents in analysis of fibrous feeds. II. A rapid method for determination of fiber and lignin. *J. Assoc. Off. Agric. Chem.* **46**, 829–835 (1963).
62. Iversen, C. M. et al. A global Fine-Root Ecology Database to address below-ground challenges in plant ecology. *New Phytol.* **215**, 15–26 (2017).
63. Birouste, M., Zamora-Ledezma, E., Bossard, C., Perez-Ramos, I. M. & Roumet, C. Measurement of fine root tissue density: a comparison of three methods reveals the potential of root dry matter content. *Plant Soil* **374**, 299–313 (2014).
64. R Core Team. *R: A Language and Environment for Statistical Computing* (R Foundation for Statistical Computing, 2022).

65. Jin, Y. & Qian, H. V.PhyloMaker: an R package that can generate very large phylogenies for vascular plants. *Ecography* **42**, 1353–1359 (2019).
66. Revell, L. J. phytools: an R package for phylogenetic comparative biology (and other things). *Methods Ecol. Evol.* **3**, 217–223 (2012).
67. Harrell, F. E. Hmisc: A package of miscellaneous R functions. CRAN https://cran.r-project.org/package=Hmisc (2014).
68. Kassambara, A. & Mundt, F. factoextra: Extract and visualize the results of multivariate data analyses. CRAN https://cran.r-project.org/package=factoextra (2020).
69. Chacón, J. E. & Duong, T. *Multivariate Kernel Smoothing and its Applications* (CRC Press, 2018).
70. Oksanen, J. et al. vegan: Community ecology package. CRAN https://cran.r-project.org/package=vegan (2022).
71. Pinheiro, J. et al. nlme: Linear and nonlinear mixed effects models. CRAN https://cran.r-project.org/package=nlme (2023).
72. Revell, L. J. Size-correction and principal components for interspecific comparative studies. *Evolution* **63**, 3258–3268 (2009).
73. Wang, M. K. Data to support: Molecular-level carbon traits underlie the multi-dimensional fine root economics space. *figshare* https://doi.org/10.6084/m9.figshare.24218970 (2024).
74. Zanne, A. E. et al. Three keys to the radiation of angiosperms into freezing environments. *Nature* **506**, 89–92 (2014).

Acknowledgements

This research was supported by the National Natural Science Foundation of China (42122054, 42192513, 42321004) to J.W.; the National Natural Science Foundation of China (32171746, 31670550) to D.K.; the Guangdong Basic and Applied Basic Research Foundation (2021B1515020082), Key Platform and Scientific Research Projects of Guangdong Provincial Education Department (2020KCXTD006), and Guangdong Provincial Key Laboratory of Soil and Groundwater Pollution Control (2023B1212060002) to J.W.; the Leading Talents of Basic Research in Henan Province to D.K.; the Natural Sciences and Engineering Research Council (NSERC) of Canada for support via the Tier 1 Canada Research Chair in Integrative Molecular Biogeochemistry to M.J.S.; a Swedish Research Council (Vetenskapsrådet) grant (2015-04214) to P.K.; the National Science Foundation: Biological Integration Institutes Grant (NSF-DBI-2021898) and Long Term Ecological Research Grant (NSF-DEB-1831944) to P.B.R.

Author contributions

M.W., D.K. and J.W. conceptualized the project. M.W., D.K., J.W., X.M., Y.W. and Q.Y. developed the methodology. D.K., J.W., M.J.S., P.K. and P.B.R. acquired funding. D.K. and J.W. administered the project. M.W., D.K. and J.W. wrote the original draft. M.W., D.K., P.K., O.J.V.-B., M.J.S., H.Z., P.B.R., J.B., N.T. and J.W. reviewed and edited the paper.

Competing interests

The authors declare no competing interests.

Additional information

Extended data is available for this paper at https://doi.org/10.1038/s41477-024-01700-4.

Supplementary information The online version contains supplementary material available at https://doi.org/10.1038/s41477-024-01700-4.

Correspondence and requests for materials should be addressed to Deliang Kong or Junjian Wang.

Peer review information *Nature Plants* thanks J. Aaron Hogan and the other, anonymous, reviewer(s) for their contribution to the peer review of this work.

Reprints and permissions information is available at www.nature.com/reprints.

Publisher's note Springer Nature remains neutral with regard to jurisdictional claims in published maps and institutional affiliations.

[1]State Environmental Protection Key Laboratory of Integrated Surface Water-Groundwater Pollution Control, School of Environmental Science and Engineering, Southern University of Science and Technology, Shenzhen, Guangdong, China. [2]Guangdong Provincial Key Laboratory of Soil and Groundwater Pollution Control, School of Environmental Science and Engineering, Southern University of Science and Technology, Shenzhen, Guangdong, China. [3]College of Forestry, Henan Agricultural University, Zhengzhou, Henan, China. [4]School of Urban Planning and Design, Peking University Shenzhen Graduate School, Peking University, Shenzhen, Guangdong, China. [5]Department of Forest Mycology and Plant Pathology, Swedish University of Agricultural Sciences, Uppsala, Sweden. [6]Department of Forest Ecology and Management, Swedish University of Agricultural Sciences, Umeå, Sweden. [7]Department of Biological Sciences, International Center for Tropical Biodiversity, Florida International University, Miami, FL, USA. [8]Environmental NMR Centre and Department of Physical and Environmental Sciences, University of Toronto Scarborough, Toronto, Ontario, Canada. [9]Department of Forest Resources University of Minnesota St, Paul, Minneapolis, MN, USA. [10]Institute for Global Change Biology and School for Environment and Sustainability, University of Michigan, Ann Arbor, MI, USA. [11]Hawkesbury Institute for the Environment, Western Sydney University, Penrith, Australia. [12]Leibniz Centre for Agricultural Landscape Research (ZALF), Müncheberg, Germany. [13]Department of Plant and Environmental Sciences, Clemson University, Clemson, SC, USA.
✉e-mail: deliangkong1999@126.com; wangjj@sustech.edu.cn

https://doi.org/10.1038/s41477-024-01700-4

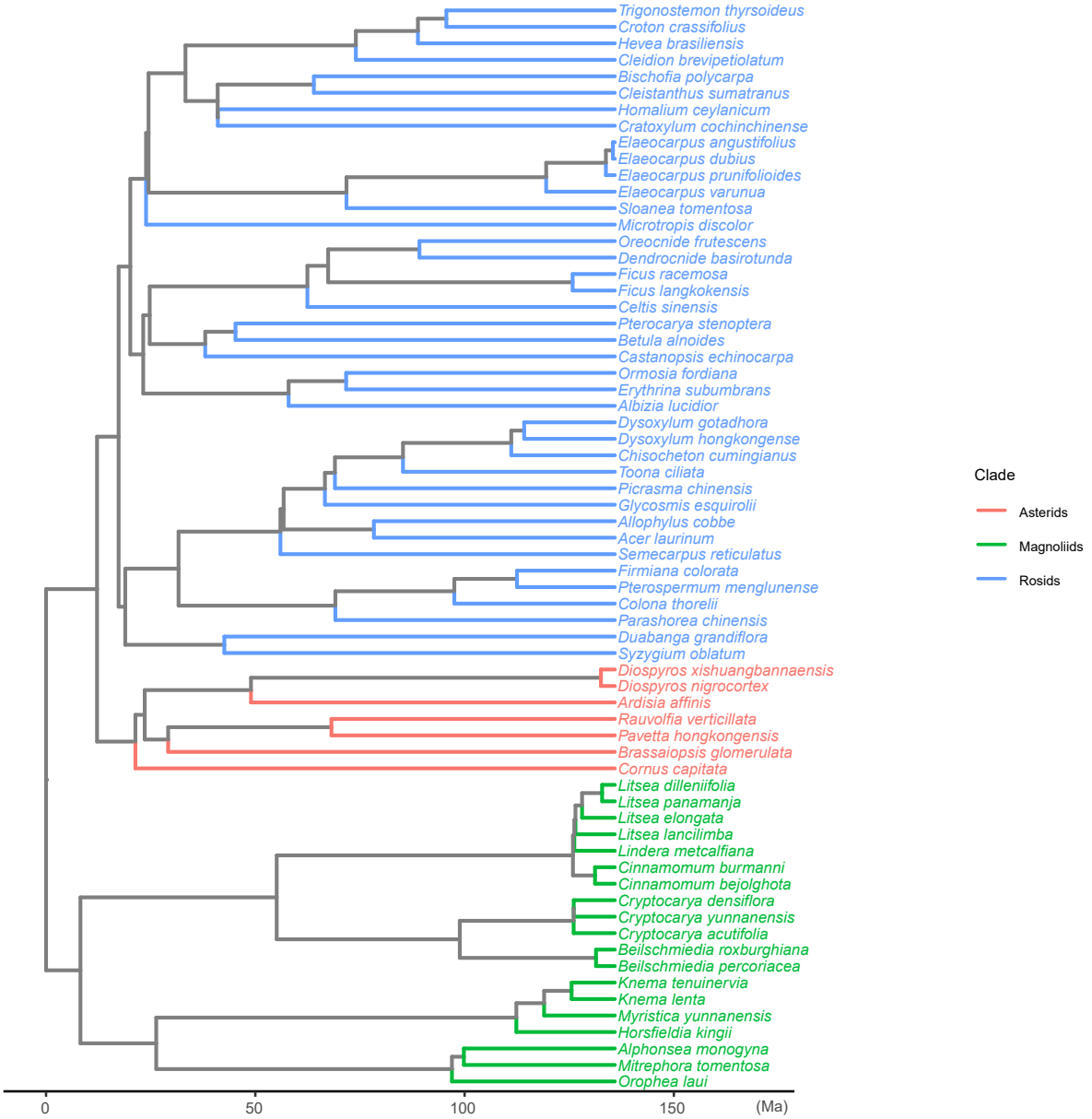

Extended Data Fig. 1 | Phylogenetic relationships for 66 tree species spanning three major angiosperm lineages (40 rosids in blue, 7 asterids in red, and 19 magnoliids in green). The phylogenetic relationships among plant species were extracted from a molecular phylogenic tree described in Zanne et al.[74].

https://doi.org/10.1038/s41477-024-01700-4

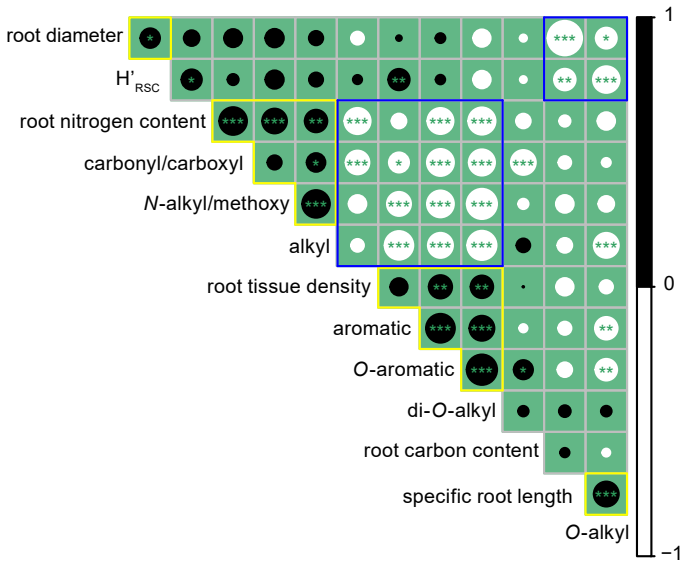

Extended Data Fig. 2 | Matrix of Pearson's correlation coefficients among 13 root traits for 66 tropical tree species. The correlation matrix is arranged in the hierarchical clustering order. A bigger circle denotes a stronger correlation. Significance level of correlations is indicated; ***, $P < 0.001$; **, $P < 0.01$; *, $P < 0.05$. Significance was tested using a two-sided t-test.

https://doi.org/10.1038/s41477-024-01700-4

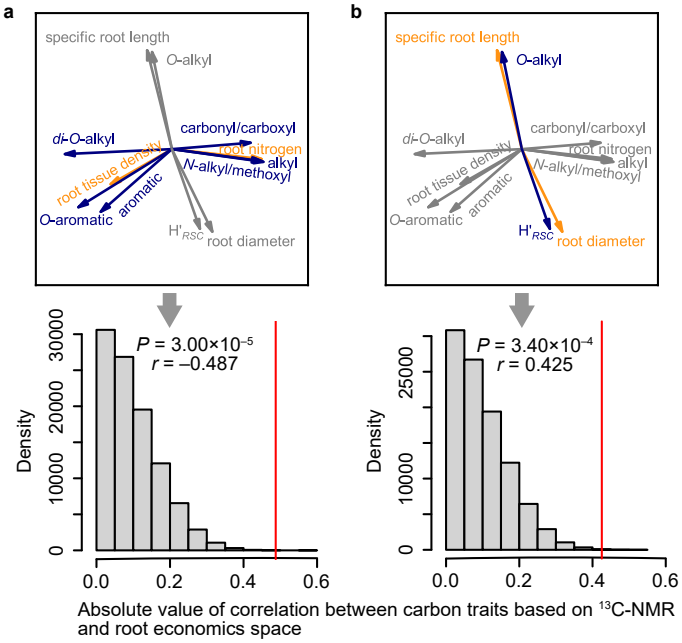

Extended Data Fig. 3 | Simulation analyses for coordination between the two-dimensional root functional trait spaces and the molecular-level root carbon traits. Observed correlations (vertical lines) relative to the distribution when scores were randomly simulated (**a**) between PC1 scores of ^{13}C-NMR-based carbon traits in the first principal component (including *O*-aromatic, aromatic, O_2-alkyl, carbonyl and carboxyl, *N*-alkyl/methoxy, and alkyl C) and PC1 scores of root economics traits in the first principal component (including root tissue density and root nitrogen concentration); (**b**) between PC2 scores of ^{13}C-NMR-based carbon traits in the second principal component (including O-alkyl and H'_{RSC}) and PC2 scores of root economics traits in the second principal component (including root diameter and specific root length). Significance was tested using a two-sided permutation test.

https://doi.org/10.1038/s41477-024-01700-4

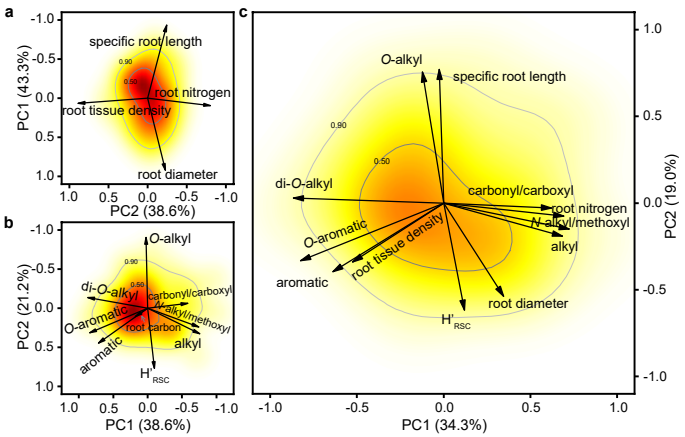

Extended Data Fig. 4 | Coordination between the two-dimensional root functional trait planes and the molecular-level root carbon traits based on phylogenetic-informed PCAs (pPCAs). (**a**) The two-dimensional root economic traits space. (**b**) Root carbon traits space, including total root carbon and molecular-level carbon traits. (**c**) Integrating both commonly-measured root functional traits and molecular-level carbon traits in the two-dimensional root functional trait space. The color gradient indicates species occurrence probability in the trait space defined by PC1 and PC2, with red indicating high occurrence and white indicating low occurrence. Contour lines indicate 0.50 and 0.90 quantiles. The commonly-measured root functional traits are root diameter, specific root length, root tissue density, and root nitrogen concentration. The carbon traits include total root carbon concentration, and 8 molecular-level carbon traits (alkyl, *N*-alkyl/methoxy, *O*-alkyl, di-*O*-alkyl, aromatic, *O*-aromatic, carbonyl/carboxyl, and structural carbon trait diversity (H'_{RSC})).

https://doi.org/10.1038/s41477-024-01700-4

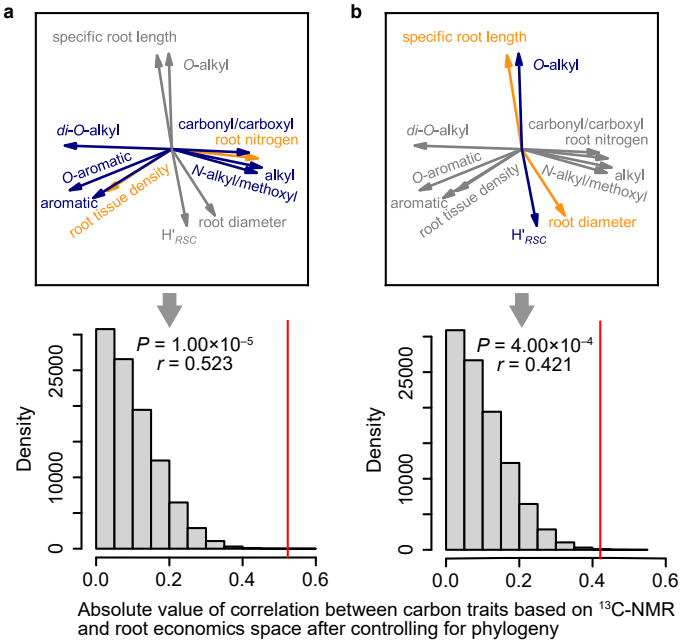

Extended Data Fig. 5 | Simulation analyses for coordination between the two-dimensional root functional trait spaces and the molecular-level root carbon traits after controlling for phylogeny. Observed correlations (vertical lines) relative to the distribution when scores were randomly simulated (**a**) between PC1 scores of ^{13}C-NMR-based carbon traits (including *O*-aromatic, aromatic, O_2-alkyl, carbonyl and carboxyl, *N*-alkyl/methoxy, and alkyl C) and PC1 scores of root economics traits (including root tissue density and root nitrogen concentration) after controlling for phylogeny, and (**b**) between PC2 scores of ^{13}C-NMR-based carbon traits in the second principal component (including *O*-alkyl and H'_{RSC}) and PC2 scores of root economics traits (including root diameter and specific root length) after controlling for phylogeny. Significance was tested using a two-sided permutation test.

https://doi.org/10.1038/s41477-024-01700-4

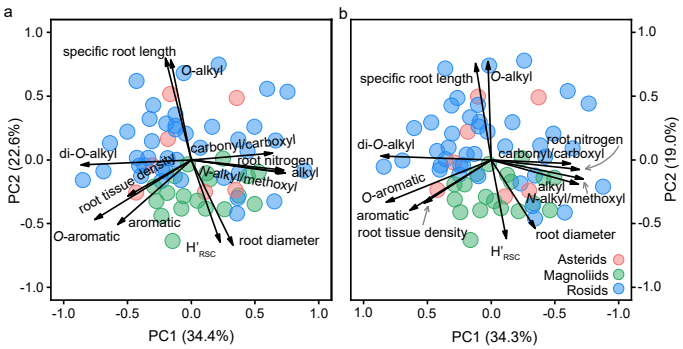

Extended Data Fig. 6 | Different species in the two-dimensional root trait space. Ordination of 66 tree species from three major clades, Asterids (in red), Magnolidds (in green) and Rosids (in blue), in the two-dimensional root trait space based on (**a**) principal component analysis and (**b**) phylogenetically-informed principal component analyses.

nature portfolio

Corresponding author(s): Junjian Wang, Deling Kong

Last updated by author(s): Apr 1, 2024

Reporting Summary

Nature Portfolio wishes to improve the reproducibility of the work that we publish. This form provides structure for consistency and transparency in reporting. For further information on Nature Portfolio policies, see our Editorial Policies and the Editorial Policy Checklist.

Statistics

For all statistical analyses, confirm that the following items are present in the figure legend, table legend, main text, or Methods section.

n/a	Confirmed	
☐	☒	The exact sample size (*n*) for each experimental group/condition, given as a discrete number and unit of measurement
☐	☒	A statement on whether measurements were taken from distinct samples or whether the same sample was measured repeatedly
☐	☒	The statistical test(s) used AND whether they are one- or two-sided *Only common tests should be described solely by name; describe more complex techniques in the Methods section.*
☐	☒	A description of all covariates tested
☐	☒	A description of any assumptions or corrections, such as tests of normality and adjustment for multiple comparisons
☐	☒	A full description of the statistical parameters including central tendency (e.g. means) or other basic estimates (e.g. regression coefficient) AND variation (e.g. standard deviation) or associated estimates of uncertainty (e.g. confidence intervals)
☐	☒	For null hypothesis testing, the test statistic (e.g. *F*, *t*, *r*) with confidence intervals, effect sizes, degrees of freedom and *P* value noted *Give P values as exact values whenever suitable.*
☐	☒	For Bayesian analysis, information on the choice of priors and Markov chain Monte Carlo settings
☒	☐	For hierarchical and complex designs, identification of the appropriate level for tests and full reporting of outcomes
☐	☒	Estimates of effect sizes (e.g. Cohen's *d*, Pearson's *r*), indicating how they were calculated

Our web collection on statistics for biologists contains articles on many of the points above.

Software and code

Policy information about availability of computer code

Data collection	Solid-state 13C NMR spectra were acquired on a Bruker AVANCE III 600 spectrometer and processed preliminarily using TopSpin 4.2.0. Root morphology parameters were acquired by root image analysis using Winrhizo software (2007 Pro version; Regent Instruments, Quebec, QC, Canada). The total nitrogen and carbon contents were determined using a Vario MACRO cube elemental analyzer (Elementar, Hanau, Germany). The contents of hemicellulose and cellulose components and lignin components were detected using a fiber analyser (ANKOM A2000i; Ankom, USA). Literature data were collected from the Fine-Root Ecology Database 3.0 (http://roots.ornl.gov).
Data analysis	We performed data analyses using some common packages in R-software (v.4.1.1), e.g. V.PhyloMaker, phytools, Hmisc, factoextra, ks, vegan(v.2.6-4), nlme.

For manuscripts utilizing custom algorithms or software that are central to the research but not yet described in published literature, software must be made available to editors and reviewers. We strongly encourage code deposition in a community repository (e.g. GitHub). See the Nature Portfolio guidelines for submitting code & software for further information.

Data

Policy information about availability of data

All manuscripts must include a data availability statement. This statement should provide the following information, where applicable:

- Accession codes, unique identifiers, or web links for publicly available datasets
- A description of any restrictions on data availability
- For clinical datasets or third party data, please ensure that the statement adheres to our policy

The data of this study are included in the article and in the Supplementary Materials and are available at figshare "https://doi.org/10.6084/m9.figshare.24218970". Literature data were extracted from Fine-Root Ecology Database 3.0 (https://roots.ornl.gov/).

Research involving human participants, their data, or biological material

Policy information about studies with human participants or human data. See also policy information about sex, gender (identity/presentation), and sexual orientation and race, ethnicity and racism.

Reporting on sex and gender	Not applicable.
Reporting on race, ethnicity, or other socially relevant groupings	Not applicable.
Population characteristics	Not applicable.
Recruitment	Not applicable.
Ethics oversight	Not applicable.

Note that full information on the approval of the study protocol must also be provided in the manuscript.

Field-specific reporting

Please select the one below that is the best fit for your research. If you are not sure, read the appropriate sections before making your selection.

☐ Life sciences ☐ Behavioural & social sciences ☒ Ecological, evolutionary & environmental sciences

For a reference copy of the document with all sections, see nature.com/documents/nr-reporting-summary-flat.pdf

Ecological, evolutionary & environmental sciences study design

All studies must disclose on these points even when the disclosure is negative.

Study description	This study proposed a conceptual framework of the two-dimensional root functional trait space including both root “classic” economic and molecular-level C traits.
Research sample	This study included sixty-six woody species in a secondary tropical seasonal rainforest. Plant species were selected based on their occurrence as a native plant in the northern edge of Southeast Asian tropical regions (except only one species, i.e., Hevea brasiliensis, is native to south American but was introduced to this area in mid-20th), their phylogeny (spanning major angiosperm lineages: Rosids, Asterids, and Magnoliids) and their root strategy (encompassing a large proportion of the variation in "fast-slow" and "collaboration" gradients of the root economics spece).
Sampling strategy	For each species, fine-root samples were selected from at least three mature plants (aged more than 30 yr). If less than three individuals were observed or easily accessible in the study site, at least 2 fine-root samples at different site of one tree were collected. This selection process effectively minimized the potential confounding effects arising from climatic, geographical, and soil variations, to ensure the representativeness and generalizability in phylogeny of the observed patterns.
Data collection	Root morphology parameters were acquired by root image analysis using Winrhizo software by Deliang Kong and Qingpei Yang. The total nitrogen and carbon contents were determined using a Vario MACRO cube elemental analyzer. Solid-state 13C NMR spectra were acquired on a Bruker AVANCE III 600 spectrometer and processed preliminarily using TopSpin 4.2.0. The contents of hemicellulose and cellulose components and lignin components were detected using a fiber analyser. These experiments were carried out by Mengke Wang, Xiaohan Mo and Yinghui Wang. Literature data were collected from the Fine-Root Ecology Database 3.0 by Mengke Wang.
Timing and spatial scale	All root samples were collected in July 2017.
Data exclusions	No data were excluded.

Reproducibility	No data were excluded.
Randomization	Plant species were randomly selected according to the rules in "Research sample". Plant individuals were randomly selected in the study site. Fine-root samples were randomly selected in one tree.
Blinding	Blinding was not relevant to this study because this study mainly focused on the trait relationship rather than species variation. Moreover, the high number of analogous samples made it impossible to infer any pattern, making blinding superfluous.

Did the study involve field work? ☒ Yes ☐ No

Field work, collection and transport

Field conditions	This site encompasses a tropical seasonal rainforest with an average annual precipitation of 1428 mm of which 80% occurs in the rainy season (May-October) and the dry season occurs during November to April and an average annual temperature of 22.5°C. Its elevation is ranging from 370 to 2400 m above sea level. The soil type prevalent in this area is brick-red soil (Oxisol), derived from yellowish sandstone of the Cretaceous period. The reserve is distinguished by its zonal vegetation types (primarily tropical rainforest and tropical seasonal rainforest) and represents the northernmost boundary of Southeast Asian tropical rainforest. Situated at the crossroads between the ancient tropical flora and the pan-Arctic flora, as well as between the East Asian and the Himalayan flora, this reserve houses a profoundly intricate biological composition and showcases an extensive array of species diversity. Within this reserve, flora with a tropical distribution accounts 83.5% of the total number of genera, and those of temperate distribution contribute 10.6% of the total genera. The reserve encompasses a variety of forest types, such as tropical rainforests, tropical seasonal rainforests, evergreen broad-leaf forests, and rubber plantations. The study was conducted within a secondary forest in the reserve after minor human disturbances, such as moderate logging for firewood, from the primary forest. Since the establishment of the National Nature Reserve in 1958, human activities have been strictly restricted, and logging has been completely avoided. Nowadays, there are still some legacies of primary forest. The forest community at the study site exhibits a vertical structure consisting of a canopy layer, shrub layer, herbaceous layer. The canopy layer, with a canopy coverage of approximately 90%, can be further divided into three sublayers. It comprises nearly 300 species, including 22 dominant species, and has an average height of 22 m with a canopy closure of 0.9. The shrub layer consists of approximately 70 species, including 8 dominant species, with an average height of 1.5 m and a coverage of 50%. In contrast, the herbaceous layer encompasses 45 species, including 5 dominant species, with an average height of 0.5 m and a coverage of 40.
Location	The study site is situated in Xishuangbanna, China (101.2 E, 21.95 N), and it falls within the Xishuangbanna National Nature Reserve (more than 2400 km2), which was established in 1958. Situated on the northern edge of Southeast Asian tropical regions, it lies within the northern tropical monsoon climatic zone.
Access & import/export	Individual authors that contribute data determined the access to the study site.
Disturbance	Sampling activities of this study was conducted under the supervision of staff in the reserve. Therefore, no disturbance was caused by the study.

Reporting for specific materials, systems and methods

We require information from authors about some types of materials, experimental systems and methods used in many studies. Here, indicate whether each material, system or method listed is relevant to your study. If you are not sure if a list item applies to your research, read the appropriate section before selecting a response.

Materials & experimental systems

n/a	Involved in the study
☒	☐ Antibodies
☒	☐ Eukaryotic cell lines
☒	☐ Palaeontology and archaeology
☒	☐ Animals and other organisms
☒	☐ Clinical data
☒	☐ Dual use research of concern
☐	☒ Plants

Methods

n/a	Involved in the study
☒	☐ ChIP-seq
☒	☐ Flow cytometry
☒	☐ MRI-based neuroimaging

Dual use research of concern

Policy information about dual use research of concern

Hazards

Could the accidental, deliberate or reckless misuse of agents or technologies generated in the work, or the application of information presented in the manuscript, pose a threat to:

No	Yes	
☒	☐	Public health
☒	☐	National security
☒	☐	Crops and/or livestock
☒	☐	Ecosystems
☒	☐	Any other significant area

Experiments of concern

Does the work involve any of these experiments of concern:

No	Yes	
☒	☐	Demonstrate how to render a vaccine ineffective
☒	☐	Confer resistance to therapeutically useful antibiotics or antiviral agents
☒	☐	Enhance the virulence of a pathogen or render a nonpathogen virulent
☒	☐	Increase transmissibility of a pathogen
☒	☐	Alter the host range of a pathogen
☒	☐	Enable evasion of diagnostic/detection modalities
☒	☐	Enable the weaponization of a biological agent or toxin
☒	☐	Any other potentially harmful combination of experiments and agents

Plants

Seed stocks	The root samples in this study were collected in Xishuangbanna, China (101.2 E, 21.95 N) in July 2017. We carefully excavated the surface soil (0–20 cm) at the base of the trees to expose the main lateral roots. We then cut root branches with intact terminal branch orders, collecting samples of the branches that included over 20 g of total fresh biomass of the first three-order roots.
Novel plant genotypes	Not applicable.
Authentication	All tree species in this study were identified by the Xishuangbanna National Nature Reserve.